Structural Eng. / Earthquake Eng. Vol. 3. No. 1, 53s-61s, April 1986
Japan Society of Civil Engineers (Proc. of JSCE No. 368/ I -5)

GENERIC FORMULATION PROCEDURE FOR LARGE DEFORMATION ANALYSIS OF STRUCTURAL ELEMENTS

By Worsak KANOK-NUKULCHAI, Akio HASEGAWA** and Fumio NISHINO****

A general Lagrangian formulation of structural finite elements is presented, in the context of nonlinear continuum mechanics. The element characteristics are 'degenerated' from 3D field equations, using kinematic characteristics of the structural member. Consistent linearization is performed to establish a Newton-Raphson solution scheme. Numerical examples are tested and the results clearly indicate the effectiveness of the present formulation.

1. INTRODUCTION

In the past decade, large deformation of common structural members such as beam, plate and shell has become a subject of increasing interest. A variety of finite elements developed for nonlinear analysis of such structures are based on classical theories. These theories, in pre-computer age, were established usually in a form suitable for hand-calculations for specific types of structures. Various assumptions and approximations with respect to global geometry and deformation of the structure were already imbedded. Disadvantages adherent to this 'classical' approach are : (a) the element application could be severely limited by the modest application scope of the underlying classical theory : (b) the element could be subjected to a higher order continuity requirement. Such elements appear to be rather complicated as well as time-consuming.

A new approach is to treat structural member as a special case of 3D continuum. Structural element is essentially 'degenerated' from 3D field equations using appropriate kinematic constraints characteristic of the structural member. The conceptual difference of this 'degeneration' approach[1),3)] from the classical one is illustrated in Fig. 1 for shell. Both approaches involve the entire process of reducing a shell-like continuum into finally a consistent surface patch of shell elements. The process uses two classes of approximation : one resulting from the finite element discretization and the other from enforcing shell assumptions. For example, a classical element for shells of a specific shape can be derived by discretizing the governing differential equations of a relevant shell theory, in which shell assumptions have already been taken into account. On the other hand, the degeneration approach directly discretizes the shell-like

* Ph. D., Asso. Prof., Asian Institute of Technology (Bangkok, Thailand), formerly Asso. Prof. of Univ. of Tokyo
** Member of JSCE, Dr. Eng., Asso. Prof., Dept. of Civil Eng., Univ. of Tokyo. (Bunkyo-ku, Tokyo)
*** Member of JSCE, Ph. D., Vice President for Academic Affairs, Asian Institute of Technology, on leave from Univ. of Tokyo

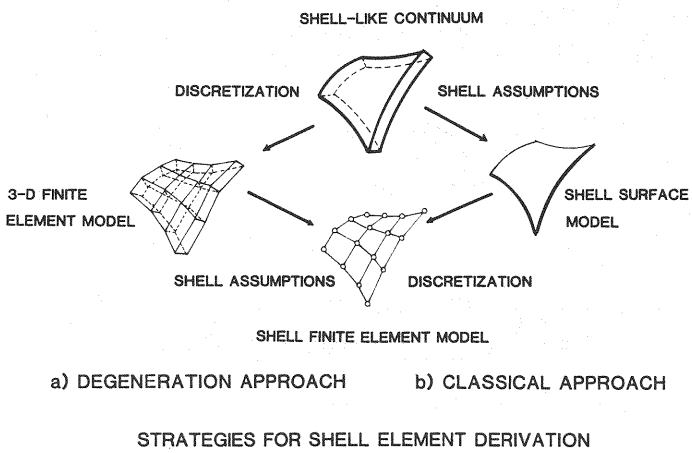

Fig. 1 Two approaches for shell element formulation.

continuum before shell assumptions are enforced at the element level in total disregard of the global form of the shell geometry. The latter approach should result in a shell element that is tied neither to any specific shell theory nor to any global form of surface geometry. Another advantage is the lower order continuity requirement on the field variables, which should normally lead to a simple formulation and a low computational cost.

In nonlinear analysis, computational cost is a prime concern due to the requirement for frequent formation of element characteristics. The use of complex but too expensive high order elements is an extravagence if one considers the uncertainty of many nonlinear material characteristics in existence. Thus, degenerate elements, being conceptually simple but rigorous, should be an ideal alternative for applications in practice.

This paper presents a generic formulation procedure for establishing degenerate structural elements for large-deformation analysis. The element characteristics are established from the balance equations in the Lagrangian mode of description.

The proposed procedure to establish an element model for a specific class of structures involves (a) appropriate selection of element geometry, nodes as well as nodal variables : (b) employment of element shape functions which incorporate all the kinematic characteristics of the applied class of structures, and (c) reduction of the three-dimensional constitutive model into a suitable form.

2. LAGRANGIAN FORMULATION OF A LARGE-DEFORMATION ELEMENT

The motion of a body B is a one-parameter family of its configuration B_t in the Euclidean space. The spatial Cartesian coordinate system $\boldsymbol{x}$ serves to describe motions of particles in the space. Another set of Cartesian coordinates $\boldsymbol{X}$, known as the reference coordinates, describes the material framework of a configuration B_0 which is employed as a deformation reference. Motion of a particle P can be given in terms of a displacement vector $\boldsymbol{u}$ from its reference position, $\boldsymbol{X}(P)$, in configuration B_0, as

$$x_j(X, t)=\delta_{jJ}X_J+d_j+u_j(X, t) \quad (1)$$

where δ_{jJ} denotes the Cartesian shifter between $\boldsymbol{x}$ and $\boldsymbol{X}$ systems and $\boldsymbol{d}$ is the position vector to the origin of $\boldsymbol{X}$ system. Throughout this presentation, upper-case and lower-case subscripts are used to differentiate between the components associated with $\boldsymbol{x}$ and $\boldsymbol{X}$ respectively. Also, a repeated index in a term implies summation over its range, according to tensor notation.

Physical principles governing the motion and thermal responses of deformable bodies include conservation of mass, balance of linear and angular momenta, balance of energy and the entropy production inequality[4]. Restricting our interest to elastic bodies under isothermal deformation, the balance of angular momentum is satisfied through symmetric propertry of stress tensor. Finally, the conservation of mass is satisfied through $\rho_t=\rho_0/J_t$ where ρ_0 and ρ_t are mass densities of the body at B_0 and B_t respectively and J_t is the determinant of the deformation gradient matrix which maps B_0 into B_t. With a constitutive model constructed to comply with the entropy production inequality, the elastodynamic problem reduces to the determination of deformation and stress responses that satisfy the balance equation of linear momentum.

The balance of linear momentum, together with constitutive equations, strain-displacement relations,

and appropriate initial and boundary conditions, constitutes an initial boundary value problem. The Galerkin weak form (or virtual work expression) of this initial boundary value problem can be used to establish the discretized equations of motion by the finite element method.

First, the local balance of linear momentum governing particle in B is expressed in Lagrangian mode[4] as

$$(S_{IJ}F_{jJ})_{,I}+\rho_0 b_j-\rho_0\ddot{u}_j=0 \quad (2)$$

in which $\boldsymbol{b}$ is the body force vector, $\boldsymbol{S}$ the second Piola-Kirchhoff stress tensor and $\boldsymbol{F}$ the deformation gradient associated with a motion from B_0 to B_t. Assuming that the motion is sufficiently smooth for differentiation, $\boldsymbol{F}$ is given by

$$F_{jJ}=\frac{\partial x_j}{\partial X_J} \quad (3)$$

The traction boundary conditions associated with the boundary surface ∂B_0 is as follows.

$$n_I S_{IJ}F_{jJ}-\hat{T}_j=0 \quad (4)$$

where $\boldsymbol{n}$ is the unit normal vector of ∂B_0 and $\hat{\boldsymbol{T}}$ is the prescribed traction acting on ∂B_0.

The Galerkin weighted residual method is applied to (2) and (4) to construct a Galerkin's weak form of the problem, i.e.,

$$G(u,\eta)=-\int_{B_0}(S_{IJ}F_{jJ})_{,I}\,\eta_j dV-\int_{B_0}(\rho_0 b_j-\rho_0\ddot{u}_j)\eta_j dV+\int_{\partial B_0}(n_I S_{IJ}F_{jJ}-\hat{T}_j)\eta_j dA \quad (5)$$

in which η denotes a weight field over B_0. One can easily recognize that (5) can be interpreted as virtual workdone if η is viewed as the virtual displacement field. Applying the Gauss-Green Theorem to the first integral leads to a corresponding canonical form of (5). If both $\boldsymbol{u}$ and η are continuous over the element domain, the Galerkin function can be written as an accumulation of individual element contributions, i.e., $G(\boldsymbol{u},\eta)=\sum_e G^e(\boldsymbol{u},\eta)$ where the canonical form of a typical G^e associated with (5) is

$$G^e(\boldsymbol{u},\eta)=\int_{B_0^e}S_{IJ}F_{jJ}\eta_{j,I}dV-\int_{B_0^e}(\rho_0 b_j-\rho_0\ddot{u}_j)\eta_j dV-\int_{\partial B_0^e}\hat{T}_j\eta_j dA \quad (6)$$

For a finite element, if n is the number of nodes in the element and $\boldsymbol{U}$ is the element nodal variables, shape functions are constructed in such a way that the three-dimensional displacement field $\boldsymbol{u}$ over the element body can be expressed in terms of $\boldsymbol{U}$ as

$$\boldsymbol{u}(\boldsymbol{X})=\sum_{a=1}^{n}N^a(\boldsymbol{X})\boldsymbol{U}^a \quad \text{for} \quad P(\boldsymbol{X})\in B_0^e \quad (7)$$

These shape functions must be established such that they incorporate all the imposed constraints to reflect the proper characteristic behaviour of the applied structure. The same set of shape functions may also be used to represent the element geometry if element isoparametry is desired.

The Galerkin method employs the weight field η which belongs to the same function space as the displacement field. In addition, η is chosen to satisfy homogeneous essential boundary conditions. Thus, η can be represented by

$$\eta(\boldsymbol{X})=\sum_{a=1}^{n}N^a(\boldsymbol{X})\boldsymbol{H}^a \quad \text{for} \quad P(\boldsymbol{X})\in \boldsymbol{B}_0^e \quad (8)$$

where $\boldsymbol{H}$ denotes element nodal values of η. Substituting (7) and (8) into (6) leads to

$$G^e(\boldsymbol{U},\boldsymbol{H})=\sum_{a=1}^{n}\sum_{b=1}^{n}H_j^b(M_{ji}^{ba}\ddot{U}_i^a+K_j^b-R_j^b) \quad (9)$$

in which the internal force vector, the mass matrix and the generalized force vector are respectively

$$K_j^b=\int_{B_0^e}S_{IJ}F_{jJ}N_{,I}^b dV \quad (10)$$

$$M_{ji}^{ba}=\int_{B_0^e}N^a N^b dV\delta_{ij} \quad (11)$$

and

$$R_j^b=\int_{\partial B_0^e}\hat{T}_j N^b dA+\int_{B_0^e}\rho_0 b_j N^b dV \quad (12)$$

Observe that superscript refers to a node number while subscript refers to a spatial basis. For example, K_j^a denotes the j-component of the internal force vector at node 'a'. Assembling all individual element contributions leads to

$$G(\boldsymbol{U},\boldsymbol{H})=\boldsymbol{H}^T[\boldsymbol{M}\ddot{\boldsymbol{U}}+\boldsymbol{K}(\boldsymbol{U})-\boldsymbol{R}]=0 \quad (13)$$

in which $\boldsymbol{H}$ is a vector of nonprescribed weight parameters associated with global nodes. Since $\boldsymbol{H}$ can be arbitrary, (13) reduces to

$$\boldsymbol{M}\ddot{\boldsymbol{U}}+\boldsymbol{K}(\boldsymbol{U})-\boldsymbol{R}=\boldsymbol{0} \quad (14)$$

which represents the system of discretized equations of motion in terms of generalized variables $\boldsymbol{U}$.

3. LINEARIZATION OF INTERNAL FORCE VECTOR

By dropping the inertia term for quasi-static analysis, (14) reduces to a nonlinear algebraic system to be solved for $\boldsymbol{U}$ corresponding to an applied load. Solving these nonlinear equations by the Newton-Raphson technique requires the linearization of the nonlinear term $\boldsymbol{K}(\boldsymbol{U})$ with respect to $\boldsymbol{U}$. A typical linearized equilibrium system associated with (14) is

$$\boldsymbol{DK}(\boldsymbol{U}_n^m)\cdot\Delta\boldsymbol{U}_n^m=\boldsymbol{R}_n-\boldsymbol{K}(\boldsymbol{U}_n^m) \quad (15)$$

where $\boldsymbol{DK}(\boldsymbol{U}_n^m)$ denotes tangent stiffness matrix about a trial displacement $\boldsymbol{U}_n^m$ (assumed at the m-th iteration for $\boldsymbol{U}_n$, the solution corresponding to the n-th load step). The iterative increment, $\Delta\boldsymbol{U}_n^m$, is computed from (15) and used to update $\boldsymbol{U}_n^m$. It is very convenient to evaluate $\boldsymbol{DK}$ from the componential form, i. e.,

$$DK_{ji}^{ba}(\boldsymbol{U}_n^m)=\frac{\partial K_j^b}{\partial U_i^a}\bigg|_{U=U_n^m} \quad (16)$$

The expression for the element tangent stiffness is obtained by substituting (10) into (16) as

$$DK_{ji}^{ba}(\boldsymbol{U}_n^m)=\int_{B_0^e}\left(\frac{\partial S_{IJ}}{\partial U_i^a}F_{jJ}N_{,I}^b+S_{IJ}\frac{\partial F_{jJ}}{\partial U_i^a}N_{,I}^b\right)dV\bigg|_{U=U_n^m} \quad (17)$$

In view of (1), (3) and (7), the deformation gradient $\boldsymbol{F}$ can be evaluated from

$$F_{jJ}=\delta_{jJ}+\sum_{a=1}^{n}N_{,J}^aU_j^a \quad (18)$$

Using the chain rule $\partial S_{IJ}/\partial U_i^a=(\partial S_{IJ}/\partial E_{KL})(\partial E_{KL}/\partial U_i^a)$ in (17), the Green strain definition $E_{IJ}=\frac{1}{2}(F_{kI}F_{kJ}-\delta_{IJ})$ and (18), the tangent stiffness can be obtained as

$$DK_{ji}^{ba}(\boldsymbol{U})=\int_{B_0^e}[F_{jJ}(\boldsymbol{U})N_{,I}^b]\left[\frac{\partial S_{IJ}}{\partial E_{KL}}(\boldsymbol{U})\right][F_{iL}(\boldsymbol{U})N_{,K}^a]dV+\int_{B_0^e}\delta_{ij}N_{,I}^aS_{IJ}(\boldsymbol{U})N_{,J}^bdV \quad (19)$$

The first term on the right-hand side of (19) constitutes an elastic tangent stiffness with the effect of finite motion included, and the other term represents the effect of initial stresses.

4. CONSTITUTIVE MODEL

So far, the formulation is valid for any material model in which $\boldsymbol{S}$ is a function of $\boldsymbol{E}$. To avoid distractions from our main scope, only the class of hyperelastic solids will be considered, of which the constitutive equation takes the form[4]

$$S_{IJ}=\rho_0\frac{\partial\psi}{\partial E_{IJ}}(\boldsymbol{E}) \quad (20)$$

where ψ is the strain energy function. For convenience, a fourth-order elasticity tensor is introduced,

$$C_{IJKL}=\frac{1}{2}\frac{\partial S_{IJ}}{\partial E_{KL}}=\frac{1}{2}\rho_0\frac{\partial^2\psi}{\partial E_{IJ}\partial E_{KL}} \quad (21)$$

from which on can show that $C_{IJKL}=C_{KLIJ}=C_{JIKL}=C_{IJLK}$. In practice, constitutive relation can be obtained by assuming ψ as a function of $\boldsymbol{E}$. From (21), if ψ is taken as a quadratic function of $\boldsymbol{E}$, all elements of $\boldsymbol{C}$ are constant parameters. This class of material constitution corresponds to the first-order theory of elasticity[4]. For isotropic, linear elastic materials under infinitesimal strains, the elasticity tensor can be

described by 2 Lame's constants, λ and μ, as

$$2C_{KLMN}=\lambda\delta_{KL}\delta_{MN}+\mu(\delta_{KM}\delta_{LN}+\delta_{KN}\delta_{LM}) \quad (22)$$

5. SPECIALIZATION TO STRUCTURAL ELEMENTS

Table 1 lists the conditions necessary for specializing the general expressions of $\boldsymbol{K}$ and $\boldsymbol{DK}$ to four classes of nonlinear structural members as shown in Fig. 2; namely (a) truss/cable element, (b) straight/curved beam element, (c) plane/membrane element and (d) plate/shell element. Some special treatments needed for bending elements (beam, plate/shell) will be noted: (1) The conventional rotational degree-of-freedom is replaced here by the relative displacement at the top fibre. Finite rotation normally requires unorthodox treatment for its coordinate transformation leading to complex expressions[3),6)] of trigonomatric functions. In this formulation, a 'top-fibre node' is used to house the relative displacement degrees-of-freedom. An appropriate set of shape functions will be established so that the displacement field over the element body can be interpolated from degrees-of-freedom at the mid-surface nodes as well as those at nodes on the top fibre. After that, a standard nonlinear continuum procedure already described can be used to formulate the characteristics of the element straightforwardly. To maintain element isoparametry and thus enable the use of the same set of shape functions for describing element geometry, relative position vectors can be input for these relative nodes.

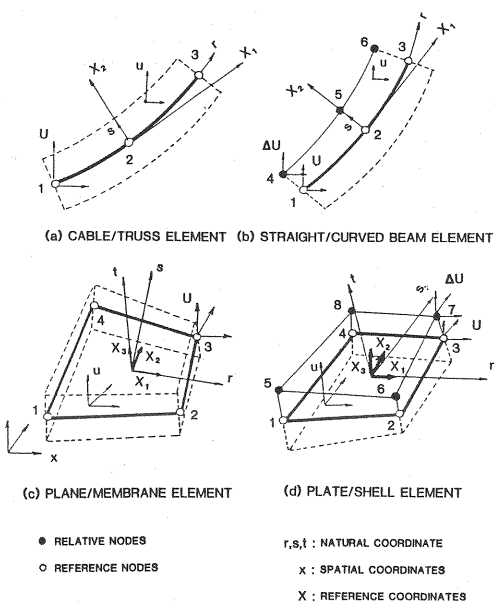

Fig. 2 Four Classes of Degenerate Elements.

(2) A fictitious coefficient ϵ is employed for the transverse normal stress-strain relationship. Theoretically, ϵ should be zero to comply with the plane-stress assumption. However, a minute value of ϵ is necessary to restrain the otherwise free thickness pinching mode due to the inclusion of the transverse relative displacement component. The range of ϵ which provides numerical stability and does not adversely affect the general element

Table 1 Four Classes of Degenerate Elements : Kinematic Field and Element Shape Functions.

TYPE OF ELEMENT	KINEMATIC CONSTRAINT	CONSTITUTIVE MODEL	ELEMENT SHAPE FUNCTIONS CONSISTENT WITH THE KINEMATIC CONSTRAINT
1. Truss/ cable element (Fig. 2a)	Axial strain is uniform over cross section	$S_{11} = E\,E_{11}$ Other S_{ij}'s except S_{11} are neglected	For a quadratic element $N^a(r,s,t) = \frac{r_a^2}{2}(r^2+r_a r)-(1-r^2)(1-r_a^2)$ $a=1,3$
2. Straight/ curved beam element (Fig. 2b)	A plane section remains plane after deformation	$\begin{Bmatrix} S_{11} \\ S_{22} \\ S_{12} \end{Bmatrix} = \begin{bmatrix} E & 0 & 0 \\ 0 & \epsilon & 0 \\ 0 & 0 & \kappa G \end{bmatrix} \begin{Bmatrix} E_{11} \\ E_{22} \\ 2E_{12} \end{Bmatrix}$ $S_{33}=S_{23}=S_{31}=0$; ϵ = fictitious coeff.	For a quadratic element $N^a(r,s,t) = \frac{1}{2} r_a^2(r+r_a r)-(1-r^2)(1-r_a^2)$ $a=1,3$ $N^a(r,s,t) = sN^{a-3}$ for relative nodes $a=4,6$
3. Plane/ membrane element (Fig. 2c)	Inplane deformation is uniform across the thickness	$\begin{Bmatrix} S_{11} \\ S_{22} \\ S_{12} \end{Bmatrix} = \begin{bmatrix} \bar{\lambda}+2\mu & \bar{\lambda} & 0 \\ \bar{\lambda} & \bar{\lambda}+2\mu & 0 \\ 0 & 0 & \mu \end{bmatrix} \begin{Bmatrix} E_{11} \\ E_{22} \\ 2E_{12} \end{Bmatrix}$	For a bilinear element $N^a(r,s,t) = \frac{1}{4}(1+r_a r)(1+s_a s)$ $a=1,4$
4. Plate/ shell element (Fig. 2d)	A straight normal remains straight after deformation	$\begin{Bmatrix} S_{11} \\ S_{22} \\ S_{33} \\ S_{12} \\ S_{23} \\ S_{31} \end{Bmatrix} = \begin{bmatrix} \bar{\lambda}+2\mu & \bar{\lambda} & 0 & 0 & 0 & 0 \\ \bar{\lambda} & \bar{\lambda}+2\mu & 0 & 0 & 0 & 0 \\ 0 & 0 & \epsilon & 0 & 0 & 0 \\ 0 & 0 & 0 & \mu & 0 & 0 \\ 0 & 0 & 0 & 0 & \mu\kappa & 0 \\ 0 & 0 & 0 & 0 & 0 & \mu\kappa \end{bmatrix} \begin{Bmatrix} E_{11} \\ E_{22} \\ E_{33} \\ 2E_{12} \\ 2E_{23} \\ 2E_{31} \end{Bmatrix}$	For a bilinear element $N^a(r,s,t) = \frac{1}{4}(1+r_a r)(1+s_a s)$ $a=1,4$ $N^a(r,s,t) = tN^{a-4}$ for relative nodes $a=5-8$ Note: $\underset{\sim}{u}(r,s,t) = \sum_{a=1}^{8} N^a(r,s,t)\underset{\sim}{U}^a$: $\underset{\sim}{U}^a \equiv \underset{\sim}{U}_{reference}$ $(a=1,4)$; $\underset{\sim}{U}^a \equiv \underset{\sim}{U}_{relative}$ $(a=5,8)$

behaviour was found[3),6)] to be between 0.1~100 times a factor of $(h^e/l^e)^2 * E$ where (h^e/l^e) is the element thickness/characteristic length aspect ratio, and E is Young's modulus.

6. COMPUTATIONAL IMPLEMENTATION

Fig. 3 shows a configuration B_t at time t and also an initial configuration denoted by B_0. During the $(n+1)st$ Newton-Raphson iteration, the configuration B_t^{n+1} is obtained by solving the linearized equilibrium system based upon the last known configuration B_t^n. Distinction should be made between the configuration about which linearization is performed (B_t^n) and the configuration that is employed for deformation reference (B_R), into which all state variables are mapped. The total Lagrangial formulation takes B_0 as B_R, where as the updated Lagrangian formulation employs B_t^n as B_R. For continua, there is no obvious, clear-cut advantage for choosing one formulation over the other. For structural members of which the generalized stress-strain relationship is not fully three-dimensionally isotropic, the total Lagrangian formulation appears to be superior. The elasticity tensor in its elementary form with respect to B_0 can be used in the formulation of tangent stiffness at all states of motion without a need for updating. Also, the reference frame $\boldsymbol{X}$ can be constructed locally to conveniently facilitate energy splitting in the evaluation of $\boldsymbol{K}$ and $\boldsymbol{DK}$, when selective reduced integration is required for 'thin' beam, plate or shell problems[7)-10)]. For this reason, the total Lagrangian formulation is generally preferable for structural elements.

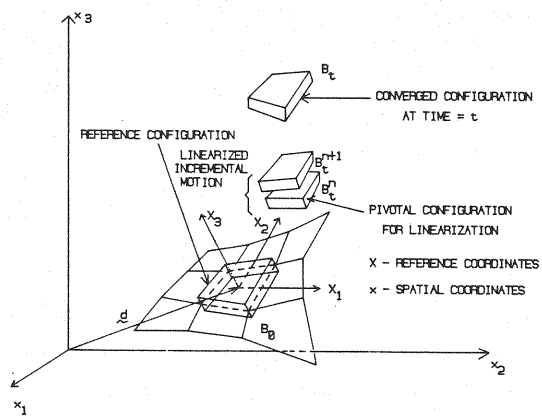

Fig. 3 Motion of a shell finite element.

For computer implementation, both $\boldsymbol{K}$ and $\boldsymbol{DK}$ of (10) and (19) can be expressed in matrix form as

$$\boldsymbol{K}^b=\int_{B_0^e}\boldsymbol{F}\,\boldsymbol{S}\,\nabla\boldsymbol{N}^b\,dV \quad (b=1,n) \qquad (23)$$

$$\boldsymbol{DK}^{ab}=\int_{B_0^e}[\boldsymbol{B}^a]^T\boldsymbol{D}\,\boldsymbol{B}^b\,dV+\int_{B_0^e}[\nabla\boldsymbol{N}^a]^T\boldsymbol{S}\,\nabla\boldsymbol{N}^b\,dV\,\boldsymbol{I} \quad (a,b=1,n) \qquad (24)$$

where $\boldsymbol{I}$ is the identity matrix; $\boldsymbol{F}\equiv[F_{iI}]$; $\boldsymbol{S}\equiv[S_{IJ}]$; $\nabla\boldsymbol{N}^b\equiv\{N^b_{,I}\}$; $\boldsymbol{B}^a$ is a matrix relating the vector of Green strain components to $\boldsymbol{U}^a$; and $\boldsymbol{D}$ is a matrix deduced from $\boldsymbol{C}$. To employ a selective reduced integration scheme, $\boldsymbol{K}$ and $\boldsymbol{DK}$ are partitioned into 2 parts : the transverse shear effect and the rest. Table 2 show the appropriate orders of Gauss quadratures for the 4 degenerate elements considered. More details should be referred to a previous paper[3)].

Table 2 Orders of Gauss Quadrature for $\boldsymbol{K}$ and $\boldsymbol{DK}$.

Element Type	Membrane/Bending Part of $\underset{\sim}{K}$ and $\underset{\sim}{DK}$	Transverse Shear Part of $\underset{\sim}{K}$ and $\underset{\sim}{DK}$
Truss/cable quadratic element (Fig. 2a)	2 * 1 * 1+ (Exact)	-
Straight/curve beam quadratic element (Fig. 2b)	2 * 2 * 1 (Exact)	2 * 2 * 1 (Exact = 3 * 2 * 1)
Plane/membrane bilinear element (Fig. 2c)	2 * 2 * 2 (Exact)	-
Plate/shell bilinear element (Fig. 2d)	2 * 2 * 2 (Exact)	1 * 1 * 1 (Exact = 2 * 2 * 2)

Note:+ The three integers (a * b * c) refer to numbers of sampling points in (r,s,t) directions as shown Fig. 2 respectively.

7. NUMERICAL EXAMPLES

Numerical examples are solved to test the effectiveness of the present formulation. All solutions are obtained by using the Newton-Raphson iterations within each load increment. The Euclidean norm of incremental displacements smaller than 10^{-4} times the current displacement norm is the criterion for convergence. The respective number of iterations required to meet this criterion is stated in each problem. All problems were solved with the FEAP macroprogramming language[11].

(1) A prestressed cable under uniform dead load (1 lb=0.453 kg ; 1 inch=2.54 cm)

The 3-node truss/cable element is employed to idealize this cable problem. The cable, with cross-sectional area=0.065 in^2 and E=2.10^7 lb/in^2, is pretensioned to 1 300 lb before the uniform dead load is imposed. Two meshes are used, one with 2 and the other with 4 elements. The solutions are presented in Table 3, which shows good agreement with the results by Jayaraman et al.[12] using the catenary cable element. About 7 iterations are required to pass the convergence criterion in each individual load step.

(2) A cantilever beam under transverse tip load

This commonly used 'test example' is solved to test the accuracy of the degenerate beam element. The analytical solution of this problem can be obtained by means of elliptic integrals. In this example, 8 degenerate beam elements are used in the mesh. The result in Table 4 agrees exceptionally well with the analytical solution[13]. In most cases, discrepancy only shows at the fourth decimal place. In average, 7 iterations are required for the convergence in a load step.

(3) Square frame subjected to two opposite point loads

A quarter of the square frame in Fig. 4(a) is modelled by 4 degenerate beam elements and a special rigid joint element, as shown in Fig. 4(b), which serves to properly transmit plane rotation at rigid joint. This rigid joint element is formed by using the penulty function to enforce the continuity of the tangential components of the top-node relative displacements of the two connecting elements as shown in Fig. 4(b). This penulty function is in the form $1/2\ \alpha(U_n^J/h^J - U_n^I/h^I)^2$ in which α can be intepreted as a "joint modulus". An artificially large magnitude of α is required to signify the high rigidity of the joint. Analytical solution[13] for this problem is also available by elliptic integrals. Despite the crude mesh, the solution agrees very well with the analytical solution as shown in Fig. 4(c).

Table 3 Vertical Displacement (in.) of the Cable Midspan vs. Uniform Load.

Uniform Load (lb)	Present Solutions		Jayaraman et al.[12] solution
	2 elements	4 elements	
0.02	131.60	131.61	131.63
0.06	234.16	234.17	234.19
0.10	292.63	292.71	292.79
0.14	335.74	335.93	336.03
0.18	370.63	370.92	371.13

(Note: 1lb=0.453kg and 1inch=2.54cm)

Table 4 Tip Deflections of the Cantilever Beam by 8 Quadratic Beam Elements versus Analytical Large Deflection Solution[13].

Load	Vertical Displ. (w/L)		Horizontal Displ. (u/L)		End Rotation (radians)	
PL^2/EI	Exact	Present FEM	Exact	Present FEM	Exact	Present FEM$^+$
1.0	.30172	.3016	.05643	.0564	.46135	.4613
2.0	.49346	.4931	.16064	.1605	.78175	.7815
3.0	.60325	.6026	.25442	.2540	.98602	.9857
4.0	.66996	.6691	.32894	.3284	1.12124	1.1210
5.0	.71379	.7027	.38763	.3869	1.21537	1.2151
6.0	.74457	.7433	.43459	.4337	1.28370	1.2834
7.0	.76737	.7660	.47293	.4720	1.33496	1.3347

Note $^+$ Values of rotations are recomputed from relative displacements.

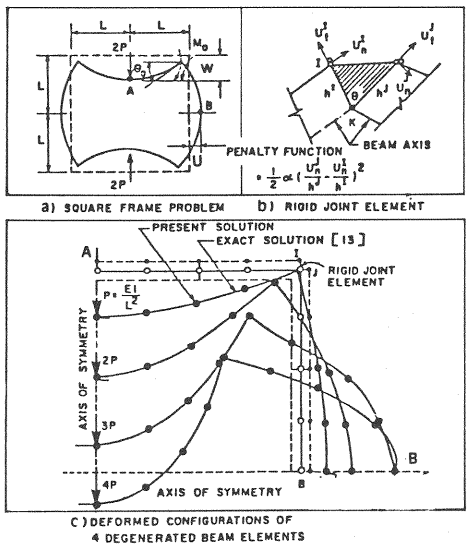

Fig. 4 Deformaion of a Square Frame.

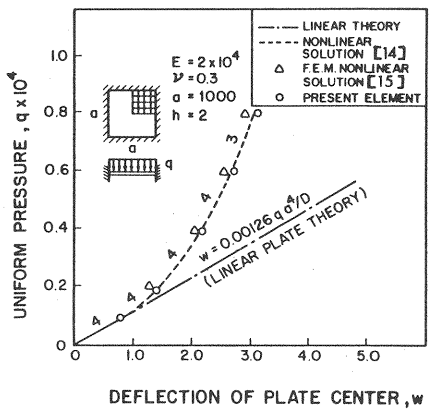

(a) Load vs. Deformation

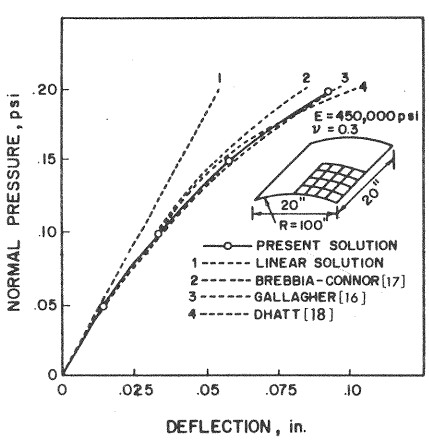

Fig. 6 Load vs. Central Deflection of Cylindrical Shell. (1 lb=0.453 kg and 1 inch=2.54 cm)

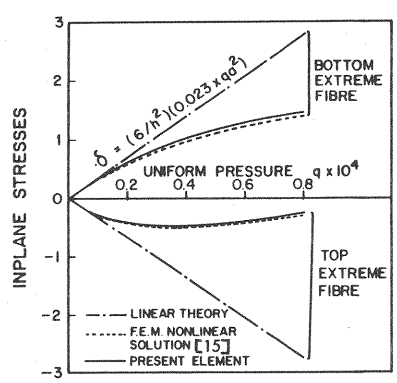

(b) Plate Stresses, Extrapolated from Gauss Points

Fig. 5 Results of Square Clamped Plate under Uniform Pressure. (Force and length units are kg and mm respectively)

(4) Square clamped plate subjected to a uniform pressure

Fig. 5 shows a 16 degenerate plate/shell element model of a quadrant of the square clamped plate. Finite deflection of the plate center is plotted versus the magnitude of uniform pressure for comparison with other solutions. The present solution shows better agreement with the analytical solution[14] than the solution of 16 cubic plate elements, reported by Kawai et al.[15] The extreme fibre stresses are also plotted in Fig. 5.

(5) A cylindrical shell subjected to normal pressures

In this problem, 16 degenerate plate/shell elements are employed for a quadrant of a cylindrical shell shown in Fig. 6. Four iterations are needed in each load step to pass the convergence criterion. In the same figure, the present solution is compared with those due to Gallagher[16], Brebbia et al.[17] and Dhatt[18]. The comparison shows overall good agreement between the present solution and Gallagher's solution.

8. CONCLUSIONS

Highlight of the present formulation for large deformation analysis of structural elements is its rigorous as well as straightforward procedure. The formulation is consistent with physical principles governing the

motion of deformable bodies. The total Lagrangian mode of description is chosen because of its efficiency in establishing the structural element characteristics. Tests of numerical examples indicate that the present formulation is very effective. The resulting degenerate elements for truss/cable, beam, plate/shell structures are believed to be economic, versatile and yet very competitive in accuracy for large deformation analysis.

9. ACKNOWLEDGEMENTS

The generic formulation presented in this paper is the generalization of the formulation presented earlier for shells[3], to be applicable to other structural elements. This paper was prepared during the first author's sabbatical leave at the University of Tokyo in 1984-85.

REFERENCES

1) Ahmad, S., Irons, B.M. and Zienkiewicz, O.C. : Analysis of thick and thin shell structures by curved finite elements, Int. J. Numer. Meth. Engng., Vol. 3, pp. 275~290, 1971.
2) Bathe, K.J., Ramm, E. and Wilson, E.L. : Finite element formulations for large deformation dynamic analysis, Int. J. Numer. Meth. Engng., Vol. 9, pp. 353~386, 1975.
3) Kanok-Nukulchai, W., Taylor, R.L. and Hughes, T.J.R. : A large deformation formulation for shell analysis by the finite element method, Computers and Structures, Vol. 13, pp. 19~27, 1981.
4) Eringen, A.C. : Continuum Physics, Vol. I and II, Academic Press, New York, 1974.
5) Argyris, J.H., Dunne, P.C., Malejannakis, G.A. and Schelkle, E. : A simple triangular facet shell element with application to linear and non-linear equilibrium and elastic stability problems, Comput. Meth. Appl. Mech. Engng., Vol. 10, No. 3, pp. 371~403, 1977.
6) Kanok-Nukulchai, W. and Sze, K.H. : An accurate degenerate beam element for large deformation analysis, Proc. of the International Conference on Finite Element Methods, Shanghai, China, pp. 727~733, August 26, 1982.
7) Zienkiewicz, O.C., Taylor, R.L. and Too, J.M. : Reduced integration technique in general analysis of plates and shells, Int, J. Numer. Meth. Engng., Vol. 3, pp. 275~290, 1971.
8) Hughes T.J.R., Cohen, M. and Haroun, M. : Reduced and selective integration techniques in the finite element analysis of plates, Nuc 1. Engng. Design, Vol. 46, pp. 203~222.
9) Hughes, T.J.R., Taylor, R.L. and Kanok-Nukulchai, W. : A simple and efficient finite element for plate bending, Int. J. Numer. Meth. Engng., Vol. 11, pp. 1629~1534, 1977.
10) Kanok-Nukulchai, W. : A simple and efficient finite element for general shell analysis, Int. J. Numer. Meth. Engng., Vol. 14, pp. 179~200, 1979.
11) Zienkiewicz, O.C. : The finite element method, 3 rd edn., Mcgraw-Hill, London, 1977.
12) Jayaraman, H.B. and Knudson, W.C. : A curved element for the analysis of cable structures, Computers and Structures, Vol. 14, pp. 325~333, 1981.
13) Mattiasson, K. : Numerical results from large deflection beam and frame problems analysed by means of elliptic integrals, Int. J. Numer. Meth. Engng. Vol. 17, pp. 145~154, 1981.
14) Way, S. : A laterally loaded clamped square plate with large deformation, Proc. 5 th Int. Congress Appl. Mech., Cambridge, Mass., 1938.
15) Kawai, T. and Toshimura, N. : Analysis of large deflection of plates by the finite element method, Int. J. Numer. Meth. Engng., Vol. 1, pp. 123~133, 1969.
16) Gallagher, R.H. : The finite element method in shell stability analysis, Computers and structures, Vol. 3, pp. 543~557, 1973.
17) Brebbia, C. and Connor, J. : Geometrically nonlinear finite element analysis, J. of Engineering Mechanics Division, ASCE, Vol. 95, No. EM 2, pp. 463~483, 1969.
18) Dhatt, G.S. : Instability of thin shells by the finite element method, Proc. of Symp. Int. Assc. Shell Structure, Vienna, 1970.

(Received April 19 1985)